Journal of Molecular Structure 1102 (2015) 275–284

Contents lists available at ScienceDirect

Journal of Molecular Structure

journal homepage: http://www.elsevier.com/locate/molstruc

Determination of reaction mechanisms and rates involving SO and NO radicals

Manoj Wijesingha, Asiri Nanayakkara*

Physical and Computational Sciences Research Unit, Institute of Fundamental Studies, Kandy, Sri Lanka

ARTICLE INFO

Article history:
Received 3 July 2015
Received in revised form
30 August 2015
Accepted 31 August 2015
Available online 2 September 2015

Keywords:
Rate constants
SONO
NOSO
Ab initio
Transition-state theory
Single-bubble sonoluminescence

ABSTRACT

Reaction rates and mechanisms involving radicals SO and NO are studied using ab initio electronic structure methods and transition-state theory calculations for the temperature range 200 K–2000 K. The molecules involved in these reactions are optimized at CCSD levels with basis set cc-PVTZ. The potential energy surface is determined computationally by MP2/6-31G(d,p) method. Moreover CCSD/cc-PVTZ levels of theory are employed to locate stationary points, which are then characterized by calculation of vibrational frequencies to locate the transition states.

In this investigation, we find that the possible products in the ground state consist of cis-SONO, SNO_2, trans-SONO, cis-NOSO, t-NOSO, NSO_2, cis-OSNO, trans-OSNO, S + NO_2 and N + SO_2. All intermediate states of the reaction SO + NO are positive energy of formation relative to the reactants. According to the reaction profiles of SO + NO, the molecular structures of the reactants are shifted to S + NO_2 (49.02 kcal/mol) and N + SO_2 (25.22 kcal/mol) through four transition structures and shifted to trans-OSNO (13.39 kcal/mol) via three transition structures. The rates calculated with variational transition state theory show that for the temperature range 200 K–2000 K, three parameter Arrhenius equation produces the most accurate reaction rates.

1. Introduction

Reactions involving sulfur oxide radical (SO) and nitric oxide radical (NO) are very important in atmospheric and combustion chemistry [1,2]. Further, the reaction rates of (a), (b) and (c) (shown below) play a role in determining the maximum temperature at the last stage of the bubble collapse in Sonoluminescence (SBSL) [3] in Sulfuric acid. During the collapse of sonoluminescence bubble, many radical reactions take place due to high temperatures and pressures occurred inside the bubble. Moreover, SO spectral lines have been observed in the SBSL spectrum [4] indicating the presence of SO radical in the bubble at the last stage of the collapse. When the bubble contains air (i.e. N_2, O_2, Ar and H_2O vapor) reactions involving SO and NO radicals take place and they influence the maximum temperature of the bubble [5].

Experimental and computational investigations carried out so far on reactions involving SO + NO are only for low temperature range 200 K–650 K [6–9]. To our knowledge, reaction rates of SO + NO for a wider temperature range such as 200 K–2000 K have never been calculated or experimentally determined. Therefore reaction rates calculated at high temperatures with best possible electronic structure methods, basis sets and transition state theory are valuable in estimating the maximum temperatures in SBSL theoretically. The reactions (a), (b), and (c) take place via intermediate complexes SONO, NOSO and OSNO molecules.

$$SO + NO \rightarrow S + NO_2 \tag{a}$$

$$SO + NO \rightarrow N + SO_2 \tag{b}$$

$$SO + NO \rightarrow OSNO \tag{c}$$

In addition to determining reactions rates, we examined possible allowed reaction pathways of SO + NO and determined the structures of possible main products and inter-mediate states such as S + NO_2, N + SO_2, SONO, SNO_2, NOSO, NSO_2 and OSNO using accurate computational chemistry techniques with a reasonably large basis set.

2. Computational method

Ab initio [10] molecular orbital theory (MO) were carried out for

---

* Corresponding author.
E-mail address: asiri@ifs.ac.lk (A. Nanayakkara).

http://dx.doi.org/10.1016/j.molstruc.2015.08.072

the reactions (a)–(c) using Gaussian 09 W [11] while reaction rates were determined by Polyrate version 2010-A [12]. The geometries of the reactants, products, intermediates, and transition states (TS) have been optimized using the couple cluster (CCSD) [10,13] method with the basis set cc-pVTZ [13]. The vibrational frequencies of the molecular systems which were calculated at the same level of theory and the basis set, have been used for the classification of stationary points, zero-point energy (ZPE) correction, and transition-state theory (TST) computations of the reaction rate constants. If only one of the calculated vibrational frequencies is imaginary, optimized states were recognized as transition states. The connections of each transition state with designated intermediates were confirmed by carrying out intrinsic reaction coordinate (IRC) calculations [14,15].

The variational transition state theory (VTST) [16,17] was utilized for the determination of thermal rate constants. The VTST optimizes the position of the dividing surface between reactant and product regions to minimize the rate constants. This minimizes the effects of recrossing, and makes the result more accurate. More detailed information on VTST can be found in Refs. [16,17]. In order to determine parameters in the Arrhenius equation, we first calculated the rate constant k for temperatures from 200 K to 2000 K in the steps of 50 K (i.e. 200 K, 250 K, 300 K … .) using VTST. Then the pre-exponential factors and activation energies of reactions (a), (b) and (c) are determined by using two and three parameter fitting expressions [18];

$$k = A\exp\left[\frac{-E_a}{RT}\right] \tag{1}$$

$$k = A\left[\frac{T}{298}\right]^{\alpha}\exp\left[\frac{-E_a}{RT}\right] \tag{2}$$

where k and E_a are the rate constant and the activation energy respectively. R is the universal gas constant and T is the temperature in Kelvin. The pre-exponential factor A and the parameter α are determined by least square fitting.

3. Results and discussion

(A) Reaction pathways and potential energy surfaces

In this investigation, we search for possible reaction channels involving the molecules SO (C_V) and NO (C_V) and study the formation of cis-SONO (C_S), trans-SONO (C_S), SNO_2 (C_S), cis-NOSO (C_S), t-NOSO (C_1), NSO_2 (C_S), cis-OSNO (C_S) and trans-OSNO (C_S) intermediate minimum electronic structures as well as products of $S + NO_2$ (C_{2V}), $N + SO_2$ (C_{2V}). All minimum structures, reactants and products illustrated in Fig. 1 are determined at CCSD/cc-pVTZ levels of the theory. The Table 1 shows the ab initio geometries of all the minimum molecular structures of the reaction. The available experimental geometries are given in parenthesis. All transition structures of the reactions (a), (b) and (c) are shown in Fig. 2 and the corresponding geometries are included in the Table 2.

In the reaction (a), all transition structures are planner except the transition structure TS2 between cis-SONO and trans-SONO. TS1 and TS3 are the transition structures of the oxygen atom of SO attacking the nitrogen atom of NO to form cis-SONO and trans-SONO. Further, there are two possible paths connecting reactants and trans-SONO. The first path takes the route over the transition states TS1 and TS2 to reach trans-SONO via Cis SONO. The other one is a direct path through the transition state TS3. The transition structure between trans-SONO and SNO_2 could not be obtained at CCSD level with the basis set cc-pVTZ. The optimized molecular structure had two imaginary frequencies instead of one and hence, the structure is not a true transition structure at the level of CCSD/cc-pVTZ. However, Chen et al. [7] and Thompson et al. [8] have studied the transition structure between trans-SONO and SNO_2 by using the B3LYP/cc-pVTZ and QCISD/6-311G(d) levels respectively. Using these methods with corresponding basis sets, we also obtained the transistion structure between trans-SONO and SNO_2. In the reaction (b), all transition structures are not planner except TS5 and TS7. The molecular structure, t-NOSO is formed via the TS5 and TS6. Note that the minimum structure t-NOSO is not the trans isomer of NOSO since the dihedral angle of the t-NOSO is not 180° (It is 148.7° degrees). From t-NOSO, there are two possible reaction channels to form S + NO2; one via TS8 and the other takes the route through the TS7 transition state and the NSO2 minimum structure. All transition structures are planner in the reaction (c). The reactants can shift to trans-OSNO directly via the TS11 while cis-OSNO is formed via transition state TS9. Further cis-OSNO and trans-OSNO can transform between each other through the transition state TS10. Two conformers of cis-SONO and trans-SONO can transform between each other through TS2 by rotating about their central bond and varying the dihedral angle between the side groups of SO and NO molecules. Further, the two conformers of cis-NOSO and t-NOSO are also able to transform between each other through TS6 by similar means. Likewise, cis-OSNO can become trans-OSNO or vise-versa through TS9 by the same rotations. On the other hand, the transition between cis and trans OSNO is different from the above and the transformation can take place via the route of swing to the NO group. Moreover, the bond angle of SNO in TS9 is 172.1° and it is 39.1° and 40.5° larger than the same in the cis-OSNO and trans-OSNO isomers respectively.

Potential energy surface (PES) [19,20] of the molecule $S{-}O_1{-}N{-}O_2$, was obtained by varying the $S{-}O_1$ and the $O_1{-}N$ bond lengths at MP2/6-31G(d,p) level. By varying the bond distances of $N{-}O_1$ and $O_1{-}S$ of $N{-}O_1{-}S{-}O_2$ molecule, another PES was obtained with the same method and the basis set. The contour plot of the PES between the reactants of SO + NO and the products of $S + NO_2$ was computed at MP2 level with 6-31G(d,p) level and is shown in Fig. 3. In the interaction region, the trans-SONO minimum is clearly identifiable. It is separated by two barriers from the reactants SO + NO and the products $S + NO_2$. Further, TS3 is clearly located between the reactants and the trans-SONO while TS4 is located between trans-SONO and the products. The contour plot in Fig. 4 shows the potential energy surface for the reactants SO + NO and the product $N + SO_2$. The minimum structure t-NOSO is clearly recognizable and the TS5 is the barrier between the reactants and inter-medium state as shown.

Table 3 lists the harmonic vibrational frequencies of the minimum and transistion structures. The experimental frequencies [21,22] of some molecular structures are given within the brackets.

NO and SO diatomic molecules each has single frequency while NO_2 and SO_2 molecules each has three frequencies corresponding to two bond lengths and one angle as shown in Table 3. Each of the other molecules considered in this investigation such as SONO, NOSO, OSNO, SNO_2, and NSO_2 has six degrees of freedom (three bond lengths, two angles and one dihedral angle) and six corresponding vibrational frequencies are shown in the table. These are real frequencies. As shown in Table 3, the five of the frequencies corresponding to eleven transition states are real and the other is pure imaginary. ZPEs of all molecular structures in the reactions (a), (b) and (c) are shown in the Table 4 and experimental values [21,22] are tabulated within the brackets. The heats of the reactions and barrier heights with the ZPE corrections are tabulated in the Table 5 which were calculated using the electronic energy of the molecular system with ZPE according to (3).

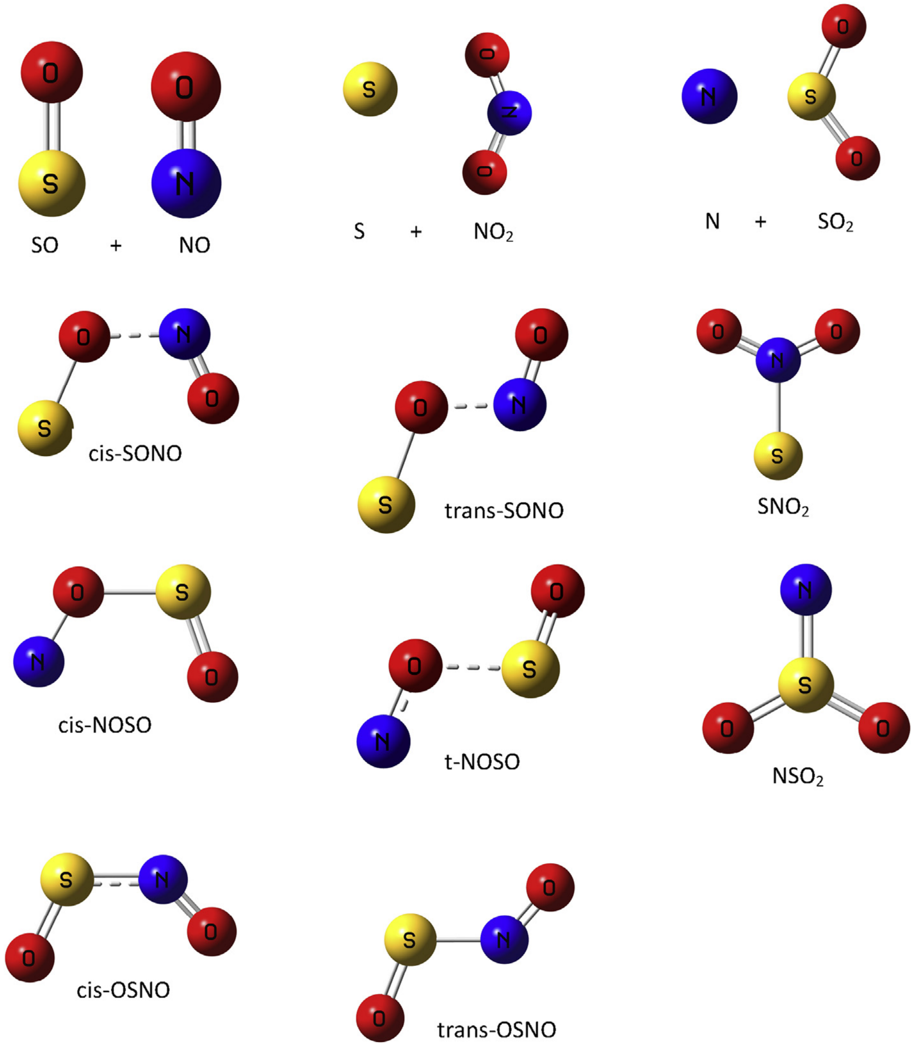

Fig. 1. The structures of local minimum involved in the reaction of SO + NO optimized by CCSD/cc-pVTZ.

$$E_{relative} = E_P - E_{reac\ tants} \quad (3)$$

where E_P is the energy of a product or a TS. The relative energies of the reactions between SO and NO as shown in Fig. 5 are approximately 16 kcal/mol for both cis-SONO and trans-SONO isomers. Compared to the cis-isomer, the relative energy of the trans isomer is little bit higher and the energy difference between cis and trans isomers of SONO is 0.68 kcal/mol at the levels of CCSD. While the isomerization of cis-SONO to trans-SONO readily takes place via TS2 structure which is having more than 16 kcal/mol of energy at the CCSD levels with respect to it's reactants, the barrier height of cis-trans isomerization is 7.06 kcal/mol. The barrier height of reactants to cis isomer is 16.62 kcal/mol which is less than 0.03 kcal/mol relative energy of the trans isomer. The largest barrier height of this reaction is encountered during the transition from trans isomer to S + NO_2 which is 54.97 kcal/mol, therefore it is the highest endothermic segment of this reaction. The low energy barrier of the reaction between cis- and trans-isomers seems to indicate a fast interconversion between these two structural isomers. As we mentioned earlier, there is a transition state between S + NO_2 and SNO2 with a single imaginary frequency at B3LYP/cc-pVTZ and QCISD/6-311G(d) levels of the theory. But at the CCSD/cc-pVTZ level, two frequencies of this state became pure imaginary and

Table 1
Geometries (bond lengths(R)/Å, bond angles (θ)/degrees, dihedral angles (τ)/degree) of the stable conformations for SO + NO reaction in the level of CCSD/cc-pVTZ.

CCSD/cc-pVTZ		CCSD/cc-pVTZ		CCSD/cc-pVTZ	
cis-SONO		cis-NOSO		cis-OSNO	
R_{SO}	1.600	R_{OS}	1.463	R_{OS}	1.463
R_{ON}	1.608	R_{SO}	1.700	R_{SN}	1.606
R_{NO}	1.135	R_{ON}	1.302	R_{NO}	1.208
θ_{NOS}	114.6	θ_{OSO}	109.2	θ_{NSO}	115.0
θ_{ONO}	112.2	θ_{NOS}	119.6	θ_{ONS}	132.9
τ_{SONO}	0.0	τ_{NOSO}	0.0	τ_{OSNO}	0.0
trans-SONO		t-NOSO		trans-OSNO	
R_{SO}	1.623	R_{OS}	1.464	R_{OS}	1.461
R_{ON}	1.535	R_{SO}	1.776	R_{SN}	1.618
R_{NO}	1.144	R_{ON}	1.272	R_{NO}	1.207
θ_{NOS}	111.2	θ_{OSO}	106.5	θ_{NSO}	111.6
θ_{ONO}	108.8	θ_{NOS}	111.2	θ_{ONS}	131.6
τ_{SONO}	180.0	τ_{NOSO}	148.7	τ_{OSNO}	180.0
SNO_2		NSO_2		NO_2	
R_{SN}	1.761	R_{NS}	1.527	R_{ON}	1.187 (1.193)
R_{NO}	1.206	R_{SO}	1.430	R_{NO}	1.187 (1.193)
R_{NO}	1.206	R_{SO}	1.430	θ_{ONO}	134.8 (134.1)
θ_{SNO}	115.9	θ_{NSO}	118.9		
θ_{ONO}	128.2	θ_{OSO}	122.1	SO_2	
τ_{SONO}	180.0	τ_{NOSO}	180.0	R_{OS}	1.439 (1.432)
				R_{SO}	1.439 (1.432)
NO		SO		θ_{ONO}	118.6 (119.5)
R_{NO}	1.147(1.154)	R_{SO}	1.490		

hence it was not possible to find a minimum energy path between S + NO_2 and SNO2 with an IRC calculation. Therefore the energy level of SNO2 is not shown in the Fig. 5. The calculated energy of the product SNO_2 is 23.73 kcal/mol relative to the reactants of SO + NO.

The energies of cis-NOSO and t-NOSO as shown in Fig. 6 are higher than their reactants by 33.03 kcal/mol and 43.72 kcal/mol respectively. TS5 energy is 10.46 kcal/mol higher compared to the cis isomer and 0.23 kcal/mol less compared to t-NOSO. The conversion of cis-NOSO to t-NOSO happens *via* TS6 which has 2.67 kcal/mol more energy than t-NOSO. The barrier height of t-NOSO to NSO_2 is 23.96 kcal/mol and it is 19.53 kcal/mol less than the highest barrier which is found between SO + NO and cis-NOSO. The molecule NSO_2 converts to the product N + SO_2 without a barrier releasing 8.22 kcal/mol.

The molecule cis-OSNO is formed by the reaction of SO and NO via TS9 (11.39 kcal/mol). Further the minimum structure of trans-OSNO (13.39 kcal/mol) is formed via the transistion structures TS11. The interconversion of cis − trans isomerization as shown in Fig. 7 occurs via TS10 which is 10.03 kcal/mol greater compared to the cis (9.33 kcal/mol) isomer. The highest barrier height between SO + NO and the trans-OSNO is 14.09 kcal/mol. It is encounted in the path which goes over the transition state TS11. All minimum structures and transistion structures of the reaction (c) are less than 20.0 kcal/mol relative to SO + NO. Bahou and Lee [21] have investigated the infrared absorption spectra of cis-OSNO and trans-OSNO using experimental and theoretical methods. Their calculated B3LYP/aug-cc-pVTZ values for the vibrational frequencies of these two isomer are found to be helpful for validating our results.

Chen et al. [6] have studied the reaction channels of SO + NO → S + NO_2 and SO + NO → trans-OSNO reactions using B3LYP method and cc-pVTZ basis set. Thompson et al. [7] have also studied the above reaction channels and rate constants. For constructing the potential energy surfaces for SNO_2 and $S(NO_2)_2$ they have used QCISD/6-311G(d,p) theory for geometries and frequencies, followed by single-point calculations based on coupled-cluster theory. Their results were extrapolated to the complete

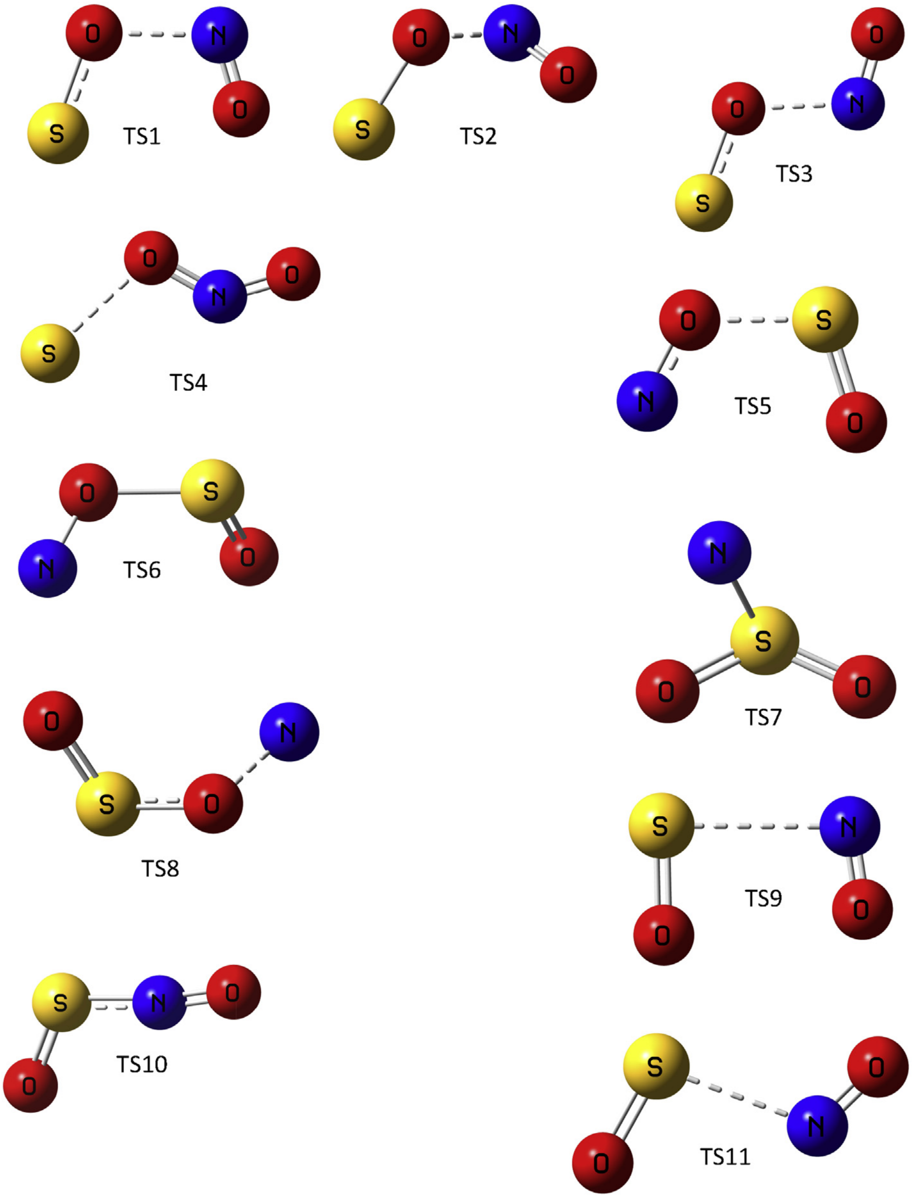

Fig. 2. The transition structures involved in the reaction of SO + NO optimized by CCSD/cc-pVTZ.

Table 2
Geometries (bond lengths(R)/Å, bond angles(θ)/degrees, dihedral angles(τ)/degree) of the transition states for SO + NO reaction in the level of CCSD/cc-pVTZ.

CCSD/cc-pVTZ		CCSD/cc-pVTZ		CCSD/cc-pVTZ	
TS1		**TS5**		**TS9**	
R_{SO}	1.556	R_{OS}	1.463	R_{OS}	1.492
R_{ON}	1.838	R_{SO}	1.852	R_{SN}	1.570
R_{NO}	1.124	R_{ON}	1.243	R_{NO}	1.141
θ_{NOS}	108.8	θ_{OSO}	106.9	θ_{NSO}	88.5
θ_{ONO}	107.2	θ_{NOS}	117.8	θ_{ONS}	98.9
τ_{SONO}	0.0	τ_{NOSO}	0.0	τ_{OSNO}	0.0
TS2		**TS6**		**TS10**	
R_{SO}	1.616	R_{OS}	1.468	R_{OS}	1.460
R_{ON}	1.578	R_{SO}	1.748	R_{SN}	1.555
R_{NO}	1.139	R_{ON}	1.293	R_{NO}	1.201
θ_{NOS}	110.4	θ_{OSO}	107.1	θ_{NSO}	115.0
θ_{ONO}	110.4	θ_{NOS}	102.3	θ_{ONS}	172.1
τ_{SONO}	83.4	τ_{NOSO}	72.1	τ_{OSNO}	180.0
TS3		**TS7**		**TS11**	
R_{SO}	1.563	R_{NS}	1.626	R_{OS}	1.490
R_{ON}	1.857	R_{SO}	1.498	R_{SN}	2.461
R_{NO}	1.128	R_{SO}	1.443	R_{NO}	1.145
θ_{NOS}	112.2	θ_{NSO}	79.6	θ_{NSO}	99.08
θ_{ONO}	107.9	θ_{OSO}	122.7	θ_{ONS}	114.4
τ_{SONO}	180.0	τ_{NOSO}	122.6	τ_{OSNO}	180.0
TS4		**TS8**			
R_{SO}	2.126	R_{OS}	1.459		
R_{ON}	1.206	R_{SO}	1.529		
R_{NO}	1.170	R_{ON}	1.807		
θ_{NOS}	107.1	θ_{OSO}	113.9		
θ_{ONO}	133.4	θ_{NOS}	112.4		
τ_{SONO}	180.0	τ_{NOSO}	−82.9		

basis set limit with cc-pV(T+d)Z and cc-pV(Q+d)Z basis sets. Chen et al. and Thompson et al. have obtained two transition states between S + NO_2, SONO and S + NO_2, SO + NO. In our research, we found only one transition state at the level of CCSD/cc-pVTZ, it is TS4. Further, Thompson et al. have observed two transition states in between cis and trans OSNO where as Chen et al. and we have found only one transition state. In this study, we have mainly focused on the reaction paths and the reaction rates of (a), (b), (c) at both low and high temperatures. In reactions involving SO and NO, at the CCSD level, the highest endothermic point is situated in the reaction (a) via the TS2.

(B) Reaction rates

For kinetic analysis [23,24], we determined the rate constants of the (a), (b) and (c) reactions which traverse through transition states TS1 to TS11 with VTST. Molecular parameters of the reactants and the transition states calculated at CCSD/cc-pVTZ are presented in Tables 1 and 2. Rate constants were computed for the temperature range of 200 K–2000 K.

In order to determine activation energies E_a and pre-exponential factors A of two and three parameter Arrhenius equation of the reaction segments (e) and (f), the rate constant data was fitted with the functions (1) and (2). The optimized values of E_a and A obtained from the fitting procedure for the above temperature range is given in Table 6, Table 7 and Table 8.

$$\mathrm{SO + NO \rightarrow TS1 \rightarrow cis\text{-}SONO} \tag{d}$$

$$\mathrm{cis\text{-}SONO \rightarrow TS2 \rightarrow trans\text{-}SONO} \tag{e}$$

$$\mathrm{SO + NO \rightarrow TS3 \rightarrow trans\text{-}SONO} \tag{f}$$

$$\mathrm{trans\text{-}SONO \rightarrow TS4 \rightarrow S + NO_2} \tag{g}$$

$$\mathrm{SO + NO \rightarrow TS5 \rightarrow cis\text{-}NOSO} \tag{h}$$

$$\mathrm{cis\text{-}NOSO \rightarrow TS6 \rightarrow t\text{-}NOSO} \tag{i}$$

$$\mathrm{t\text{-}NOSO \rightarrow TS7 \rightarrow NSO_2} \tag{j}$$

$$\mathrm{t\text{-}NOSO \rightarrow TS8 \rightarrow N + SO_2} \tag{k}$$

$$\mathrm{SO + NO \rightarrow TS9 \rightarrow cis\text{-}OSNO} \tag{l}$$

$$\mathrm{cis\text{-}OSNO \rightarrow TS10 \rightarrow trans\text{-}OSNO} \tag{m}$$

$$\mathrm{SO + NO \rightarrow TS11 \rightarrow trans\text{-}OSNO} \tag{n}$$

The energy difference between reactants and products does not affect the rate of the reaction which depends on the height of the activation barrier. By comparing reaction rates of (d), (e), (f) and (g), it can be concluded that the conversion pathway of the cis-trans SONO isomerization is faster than the pathways of the other reactions due to the low activation barrier in the isomerization reaction.

The final forms in two and three parameter fitting of Arrhenius equations for the reaction from (d) to (g) are shown bellow.

For reaction (d)

$$\mathrm{k} = 5.89 \times 10^{-12} \mathrm{e}^{-8878/\mathrm{T}} \left[\frac{\mathrm{cm}^3}{\mathrm{molecule\ s}}\right]$$

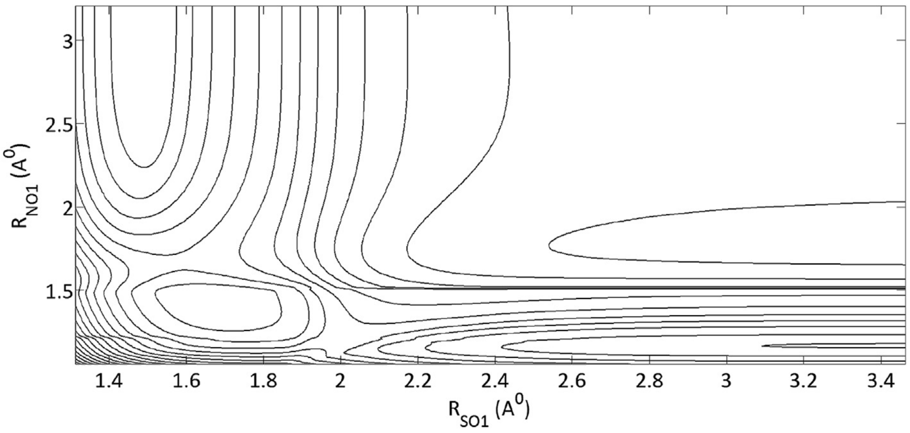

Fig. 3. A potential energy contour plot for SO + NO → S + NO_2 reaction in the level of MP2/6-31G(d,p).

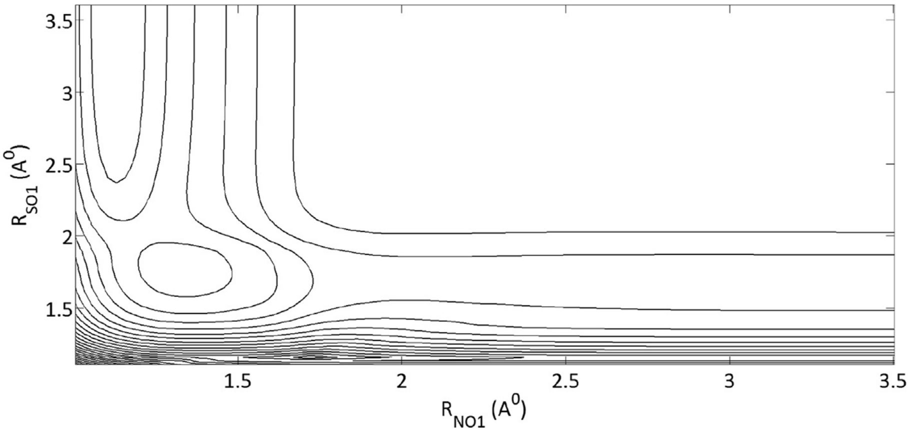

Fig. 4. A potential energy contour plot for SO + NO → N + SO_2 reaction in the level of MP2/6-31G(d,p).

$$k^1 = 1.99 \times 10^{-13}\left[\frac{T}{298}\right]^{1.855} e^{-7875/T}\left[\frac{cm^3}{molecule\ s}\right]$$

For reaction (e)

$$k = 2.24 \times 10^{13} e^{-3152/T} s^{-1}$$

$$k^1 = 2.63 \times 10^{13}\left[\frac{T}{298}\right]^{-0.0906} e^{-3201/T} s^{-1}$$

For reaction (f)

$$k = 3.02 \times 10^{-11} e^{-11303/T}\left[\frac{cm^3}{molecule\ s}\right]$$

$$k^1 = 8.13 \times 10^{-13}\left[\frac{T}{298}\right]^{1.988} e^{-10229/T}\left[\frac{cm^3}{molecule\ s}\right]$$

For reaction (g)

$$k = 6.76 \times 10^{13} e^{-27746/T} s^{-1}$$

$$k^1 = 6.76 \times 10^{13}\left[\frac{T}{298}\right]^{-0.0068} e^{-27746/T} s^{-1}$$

It was found that for the reaction from (d) to (g), the root mean square error (RMSE) of three parameter fittings is the smallest for all reaction segments. Therefore, three parameter Arrhenius equation provides the most accurate rate expressions for all the segments for the temperature range 200 K–2000 K.

By comparing rates of the segments (h) to (k), it can be concluded that the conversion pathway of the cis-NOSO isomer to t-NOSO is the fastest. It is evident from Table 7 that two parameter and three parameter reaction rate equations are having different values for E_a, A and α. Since RMSE for two parameter fitting is larger, three parameter fitting provides more accurate rate expressions. Therefore, it is concluded that reactions rates of (h) to (k) are accurately described by the three parameter Arrhenius equation. The final forms in two and three parameter fitting of Arrhenius equations for the reaction (h) to (k) are shown bellow.

for reaction (h)

$$k = 7.14 \times 10^{-3} e^{-20338/T}\left[\frac{cm^3}{molecule\ s}\right]$$

$$k^1 = 1.73 \times 10^{-3}\left[\frac{T}{298}\right]^{0.7769} e^{-19929/T}\left[\frac{cm^3}{molecule\ s}\right]$$

for reaction (i)

Table 3

Harmonic vibrational frequencies of the minimum structures and the saddle points in SO + NO at the level of CCSD/cc-pVTZ. The values inside the parentheses refer to experimental frequencies.

Minimum structures		Transition structures		
NO	cis-NOSO	TS1	TS5	TS9
1989.5 (1904)	191.5	472.9i	501.7i	500.9i
	225.9	229.5	191.4	126.2
SO	517.5	244.5	207.9	162.1
1188.2 (1151)	603.9	632.4	499.5	355.0
	1124.2	960.6	1161.8	1157.9
NO_2	1230.8	1963.8	1242.8	1893.9
780.9 (750)				
1424.4 (1318)	t-NOSO	TS2	TS6	TS10
1778.2 (1618)	104.5	208.1i	144.8i	382.5i
	254.8	252.6	246.3	275.3
SO_2	301.4	600.2	421.2	363.3
535.7 (518)	565.2	809.5	524.8	720.9
1217.2 (1151)	1138.3	870.6	1103.7	1225.6
1418.5 (1362)	1221.0	2981.4	1190.4	1658.0
Cis-SONO	NSO_2	TS3	TS7	TS11
205.3	393.7	640.4i	577.7i	576.8i
273.8	442.0	68.3	359.7	59.5
600.5	497.2	194.4	448.8	82.0
762.2	1022.2	452.3	733.9	277.5
896.5	1291.9	932.5	1012.8	1163.5
1902.6	1433.7	1968.5	1310.0	1979.4
trans-SONO	cis-OSNO	TS4	TS8	
122.4	206.7	835.1i	1144.4i	
294.5	395.6	129.2	142.0	
440.8	558.7	142.9	161.9	
700.7	721.2	766.2	487.5	
963.9	1220.9	1345.5	831.9	
2025.2	1451.1	1737.4	1245.6	
SNO_2	trans-OSNO			
274.5	276.5			
468.4	291.8			
672.7	477.1			
851.6	715.9			
1385.9	1235.3			
1661.8	1486.9			

Table 4
Zero point energies (ZPE) of SO + NO in the level of CCSD/cc-pVTZ are given in kcal/mol. The values inside the parentheses refer to experimental ZPE.

Molecule	ZPE (kcal/mol)
NO	2.84 (2.71)
SO	1.70 (1.64)
NO_2	5.69 (5.27)
SO_2	4.53 (4.33)
cis-SONO	6.63
trans-SONO	6.50
SNO_2	7.60
cis-NOSO	5.57
t-NOSO	5.12
NSO_2	7.26
cis-OSNO	6.51
trans-OSNO	6.41
TS1	5.76
TS2	7.88
TS3	5.17
TS4	5.89
TS5	4.72
TS6	4.98
TS7	5.53
TS8	4.10
TS9	5.25
TS10	6.07
TS11	5.09

$$k = 1.32 \times 10^{13} e^{-6444/T} s^{-1}$$

$$k^1 = 1.07 \times 10^{13} \left[\frac{T}{298}\right]^{0.1205} e^{-6379/T} s^{-1}$$

for reaction (j)

$$k = 5.37 \times 10^{12} e^{-13819/T} s^{-1}$$

$$k^1 = 6.76 \times 10^{12} \left[\frac{T}{298}\right]^{-0.1287} e^{-13891/T} s^{-1}$$

for reaction (k)

$$k = 7.08 \times 10^{13} e^{-18209/T} \left[s^{-1}\right]$$

$$k^1 = 4.57 \times 10^{13} \left[\frac{T}{298}\right]^{0.2316} e^{-18088/T} \left[s^{-1}\right]$$

By comparing reaction rates of the segments (l) to (n), it can be concluded that the conversion pathway of the cis-trans OSNO isomerization is faster than all the other pathways. All barrier heights of these three reactions are below 15 kcal/mol. It is evident from Table 8 that two parameter and three parameter reaction rate equations are having different values for E_a, A and α. Since RMSE for two parameter fitting is larger, three parameter fitting provides more accurate rate expressions. The final forms in two and three parameter fitting of Arrhenius equations for the reaction (l) to (n) are shown bellow.
for reaction (l)

$$k = 9.12 \times 10^{-12} e^{-3584/T} \left[\frac{cm^3}{\text{molecule s}}\right]$$

Table 5
Calculated heats of reaction and energy barriers at CCSD/cc-pVTZ levels in kcal/mol with ZPE corrections.

Reaction	Heats of reaction CCSD/cc-pVTZ (kcal/mol)	Energy barriers CCSD/cc-pVTZ (kcal/mol)
SO + NO → cis-SONO	15.96	16.82
SO + NO → trans-SONO	16.65	23.02
SO + NO → cis-NOSO	33.03	43.49
SO + NO → cis-OSNO	9.33	11.39
SO + NO → trans-OSNO	13.39	19.36
cis-SONO → trans-SONO	0.68	7.06
cis-NOSO → t-NOSO	10.69	13.36
cis-OSNO → trans-OSNO	4.06	10.03
trans-SONO → S + NO_2	8.57	54.97
SNO_2 → S + NO_2	25.29	0.0
NSO_2 → N + SO_2	8.22	0.0

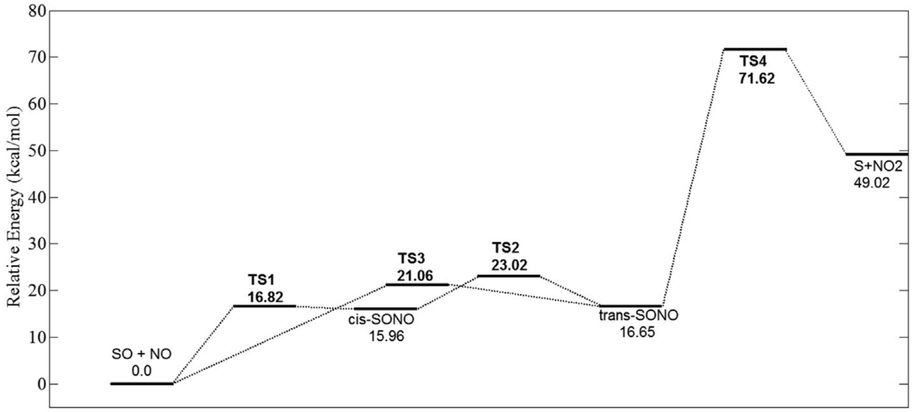

Fig. 5. The reaction profile of SONO reactions and energy calculated relative to SO + NO [CCSD/cc-pVTZ with ZPE energy].

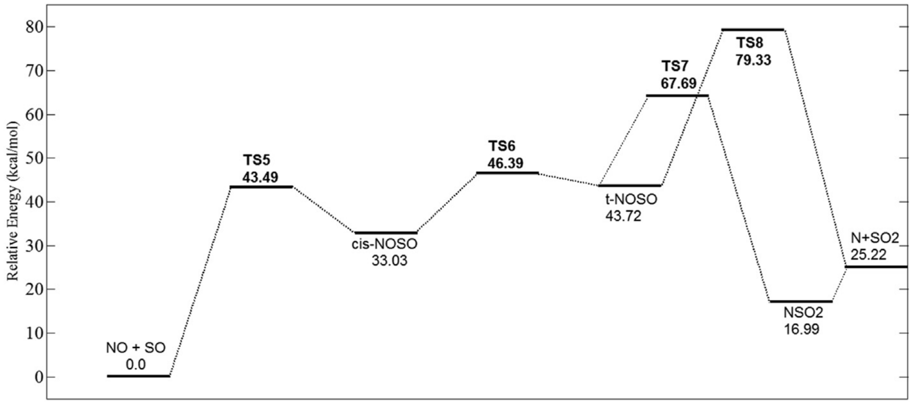

Fig. 6. The reaction profile of NOSO reactions and energy calculated relative to SO + NO [CCSD/cc-pVTZ with ZPE energy].

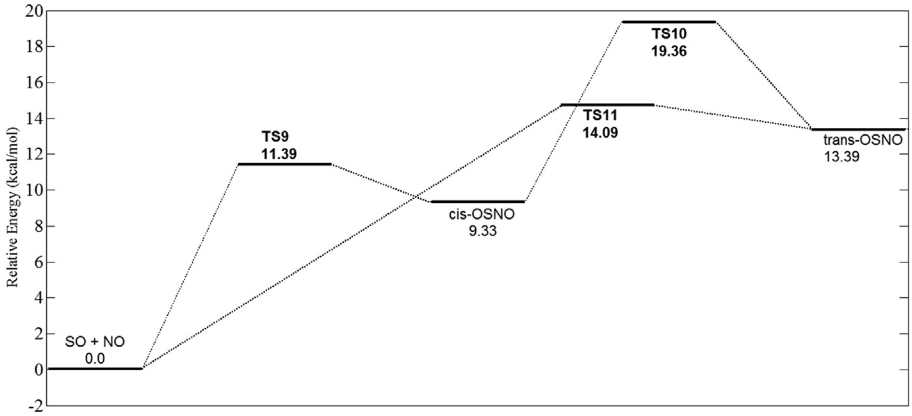

Fig. 7. The reaction profile of OSNO reactions and energy calculated relative to SO + NO [CCSD/cc-pVTZ with ZPE energy].

$$k^1 = 3.02 \times 10^{-13}\left[\frac{T}{298}\right]^{1.868} e^{-2573/T}\left[\frac{\text{cm}^3}{\text{molecule s}}\right]$$

for reaction (m)

$$k = 4.57 \times 10^{13} e^{-5692/T}\left[s^{-1}\right]$$

$$k^1 = 3.80 \times 10^{13}\left[\frac{T}{298}\right]^{0.1029} e^{-5637/T}\left[s^{-1}\right]$$

for reaction (n)

$$k = 3.39 \times 10^{-11} e^{-5289/T}\left[\frac{\text{cm}^3}{\text{molecule s}}\right]$$

Table 6
Fitting Parameters A, E_a, α, and RMSE of Arrhenius Expression for SO + NO → S + NO_2 for the temperature range 200 K–2000 K.

Reaction with temperature	Two Parameter fitting	Three Parameter fitting
SO + NO → cis-SONO (TS1)	$A = 5.89 \times 10^{-12}$ cm^3/molecule s Ea = 73820 J/mol RMSE = 0.1643	$A = 1.99 \times 10^{-13}$ cm^3/molecule s Ea = 65480 J/mol $\alpha = 1.855$ RMSE = 0.007449
cis-SONO → trans-SONO (TS2)	$A = 2.24 \times 10^{13}$ s^{-1} Ea = 26210 J/mol RMSE = 0.008116	$A = 2.63 \times 10^{13}$ s^{-1} Ea = 26620 J/mol $\alpha = -0.0906$ RMSE = 0.001289
SO + NO → trans-SONO (TS3)	$A = 3.02 \times 10^{-11}$ cm^3/molecule s Ea = 93980 J/mol RMSE = 0.1759	$A = 8.13 \times 10^{-13}$ cm^3/molecule s Ea = 85050 J/mol $\alpha = 1.988$ RMSE = 0.003556
trans-SONO → S + NO_2 (TS4)	$A = 6.76 \times 10^{13}$ s^{-1} Ea = 230700 J/mol RMSE = 0.002357	$A = 6.76 \times 10^{13}$ s^{-1} Ea = 230700 J/mol $\alpha = -0.0068$ RMSE = 0.002323

Table 7

Fitting Parameters, A, E_a, α, and RMSE of Arrhenius Expression for SO + NO → N + SO_2 for the temperature range 200 K–2000 K.

Reaction with temperature	Two Parameter fitting	Three Parameter fitting
SO + NO → cis-NOSO (TS5)	$A = 7.14 \times 10^{-3}$ cm^3/molecule s Ea = 169100 J/mol RMSE = 0.06918	$A = 1.73 \times 10^{-3}$ cm^3/molecule s Ea = 165700 J/mol $\alpha = 0.7769$ RMSE = 0.008043
cis-NOSO → t-NOSO (TS6)	$A = 1.32 \times 10^{13}$ s^{-1} Ea = 535880 J/mol RMSE = 0.01103	$A = 1.07 \times 10^{13}$ s^{-1} Ea = 53040 J/mol $\alpha = 0.1205$ RMSE = 0.002867
t-NOSO → NSO_2 (TS7)	$A = 5.37 \times 10^{12}$ s^{-1} Ea = 114900 J/mol RMSE = 0.01179	$A = 6.76 \times 10^{12}$ s^{-1} Ea = 115500 J/mol $\alpha = -0.1287$ RMSE = 0.003083
t-NOSO → N + SO_2 (TS8)	$A = 7.08 \times 10^{13}$ s^{-1} Ea = 151400 J/mol RMSE = 0.02115	$A = 4.57 \times 10^{13}$ s^{-1} Ea = 150400 J/mol $\alpha = 0.2316$ RMSE = 0.005348

Table 8

Fitting Parameters, A, E_a, α, and RMSE of Arrhenius Expression for SO + NO → OSNO for the temperature range 200 K–2000 K.

Reaction with temperature	Two Parameter fitting	Three Parameter fitting
SO + NO → cis-OSNO (TS9)	$A = 9.12 \times 10^{-12}$ cm^3/molecule s Ea = 29800 J/mol RMSE = 0.1654	$A = 3.02 \times 10^{-13}$ cm^3/molecule s Ea = 21400 J/mol $\alpha = 1.868$ RMSE = 0.00663
cis-OSNO → trans-OSNO (TS10)	$A = 4.57 \times 10^{13}$ s^{-1} Ea = 47330 J/mol RMSE = 0.01073	$A = 3.80 \times 10^{13}$ s^{-1} Ea = 46870 J/mol $\alpha = 0.1029$ RMSE = 0.005794
SO + NO → trans-OSNO (TS11)	$A = 3.39 \times 10^{-11}$ cm^3/molecule s Ea = 43980 J/mol RMSE = 0.1713	$A = 1.0 \times 10^{-12}$ cm^3/molecule s Ea = 35290 J/mol $\alpha = 1.935$ RMSE = 0.004761

$$k^1 = 1.0 \times 10^{-12}\left[\frac{T}{298}\right]^{1.935} e^{-4244/T}\left[\frac{cm^3}{molecule\ s}\right]$$

4. Summary and conclusion

The reaction rates involving SO + NO are important in atmospheric and combustion chemistry and they are valuable in simulating bubble motion in single bubble sonoluminescence and estimating the temperatures of the bubbles at the last stage of the collapse. In the current study, potential energy surfaces of SONO, NOSO and OSNO have been explored by means of ab initio molecular orbital calculations at CCSD levels. The reaction paths of SO + NO → S + NO_2, SO + NO → N + SO_2 and SO + NO → OSNO have been investigated at CCSD/cc-pVTZ level of the theory while reaction rates were determined for the temperature range 200 K–2000 K with variational transition state theory. Activation energies and pre-exponential factors of Arrhenius equation were calculated with two and three parameter fittings. The root mean square errors of these fittings have indicated that for the temperatures range $200\ K < T \leq 2000\ K$, three parameter fittings provide more accurate rate expressions.

Acknowledgment

This work was partially supported by the National Research Council of Sri Lanka under Grant No. 11-009.

References

[1] S.P.J. Rodrigues, A.J.C. Varandas, J. Phys. Chem. A 107 (2003) 5369, http://dx.doi.org/10.1021/jp0301305.

[2] W.C. Gardiner Jr., Gas-Phase Combustion Chemistry, second ed., Springer, New York, 2000.

[3] K. Yasui, T. Tuzuiti, M. Sivakumar, Y. Lida, J. Chem. Phys. 122 (2005) 224706, http://dx.doi.org/10.1063/1.1925607.

[4] D.J. Flannigan, K.S. Suslick, Phys. Rev. Lett. 95 (2005) 044301, http://dx.doi.org/10.1103/PhysRevLett.95.044301.

[5] M.P. Brenner, S.H. Hilgenfeldt, D. Lohse, Rev. Mod. Phys. 74 (2002) 425. http://dx.doi.org/10.1103/RevModPhys.74.425.

[6] M.A.A. Clyne, P.D. Whitwield, J. Chem. Soc. 75 (1979) 1327, http://dx.doi.org/10.1039/F29797501327.

[7] W.C. Chen, C.H. Yua, J. Chem. Phys. 115 (2001) 7495, http://dx.doi.org/10.1063/1.1405119.

[8] K.M. Thompson, Y. Gao, P. Marshall, Int. J. Chem. Kinet. 44 (2012) 90, http://dx.doi.org/10.1002/kin.20612.

[9] L.A. Crum, T.J. Mason, J. Reisse, K.S. Suslick, Sonochemistry and Sonoluminescence, Kluwer Publishers, Netherlands, 1999.

[10] R.A. Friesner, Proc. Natl. Acad. Sci. U. S. A. 102 (2005) 6648, http://dx.doi.org/10.1073/pnas.0408036102.

[11] M.J. Frisch, G.W. Trucks, H.B. Schlegel, G.E. Scuseria, M.A. Robb, J.R. Cheeseman, G. Scalmani, V. Barone, B. Mennucci, G.A. Petersson, H. Nakatsuji, M. Caricato, X. Li, H. P. Hratchian, A.F. Izmaylov, J. Bloino, G. Zheng, J.L. Sonnenberg, M. Hada, M. Ehara, K. Toyota, R. Fukuda, J. Hasegawa, M. Ishida, T. Nakajima, Y. Honda, O. Kitao, H. Nakai, T. Vreven, J.A. Montgomery, Jr., J.E. Peralta, F. Ogliaro, M. Bearpark, J.J. Heyd, E. Brothers, K.N. Kudin, V.N. Staroverov, T. Keith, R. Kobayashi, J. Normand, K. Raghavachari, A. Rendell, J.C. Burant, S.S. Iyengar, J. Tomasi, M. Cossi, N. Rega, J.M. Millam, M. Klene, J.E. Knox, J.B. Cross, V. Bakken, C. Adamo, J. Jaramillo, R. Gomperts, R.E. Stratmann, O. Yazyev, A.J. Austin, R. Cammi, C. Pomelli, J.W. Ochterski, R.L. Martin, K. Morokuma, V.G. Zakrzewski, G.A. Voth, P. Salvador, J.J. Dannenberg, S. Dapprich, A.D. Daniels, O. Farkas, J.B. Foresman, J.V. Ortiz, J. Cioslowski, and D.J. Fox, Gaussian, Inc., Wallingford CT, 2010.

[12] J. Zheng, S. Zhang, B.J. Lynch, J.C. Corchado, Y.Y. Chuang, P.L. Fast, W.P. Hu, Yi-P. Liu, G.C. Lynch, K.A. Nguyen, C.F. Jackels, A.F. Ramos, B.A. Ellingson, V.S. Melissas, J. Villà, I. Rossi, E.L. Coitiño, J. Pu, T.V. Albu, R. Steckler, B.C. Garrett, A.D. Isaacson, D.G. Truhlar, POLYRATE, Version 2010-A, University of Minnesota, Minneapolis, 2010.

[13] D.C. Young, Computational Chemistry, John Wiley & Sons, Inc., New York, 2001.

[14] C. Gonzalez, H.B. Schlegel, J. Chem. Phys. 90 (1989) 2154, http://dx.doi.org/10.1063/1.456010.

[15] A.G. Baboul, H.B. Schlegel, J. Chem. Phys. 107 (1997) 9413, http://dx.doi.org/10.1063/1.475238.

[16] D.G. Truhlar, A.D. Isaacson, B.C. Garrett, Generalized transition state theory, in:

M. Baer (Ed.), The Theory of Chemical Reaction Dynamics, CRC, Boca Raton, FL, 1985, p. 65.
[17] F. Ramos, B.A. Ellingson, B.C. Garrett, D.G. Truhlar, Variational transition state theory with multidimentional tunneling, in: K.B. Lipkowitz, T.R. Cundari (Eds.), Reviews in Computational Chemistry, Wiley-VCH, Hoboken, NJ, 2007, p. 125.
[18] A.M. Mebel, M.C. Lin, C.F. Melius, J. Phys. Chem. A 102 (1998) 1803, http://dx.doi.org/10.1021/jp973449w.
[19] D.G. Truhlar, The potential energy surface, in: R.A. Mayers (Ed.), The Encyclopedia of Physical Science and Technology, Academic Press, New York, 2001, p. 9.
[20] H.B. Schlegel, WIREs Comput. Mol. Sci. 1 (2011) 790, http://dx.doi.org/10.1002/wcms.34.
[21] National Institute of Standard and Technology, NIST Chemistry WebBook. Available from:http://webbook.nist.gov/chemistry
[22] M. Bahou, Y.P. Lee, J. Chem. Phys. 115 (2001) 10694, http://dx.doi.org/10.1063/1.1418253.
[23] W.H. Green Jr., C.B. Moore, W.F. Polik, Annu. Rev. Phys. Chem. 43 (1992) 591, http://dx.doi.org/10.1146/annurev.pc.43100192.003111.
[24] A.F. Ramos, J.A. Miller, S.J. Klippenstein, D.G. Truhlar, Chem. Rev. 106 (2006) 4518, http://dx.doi.org/10.1021/cr050205w.